



# Nanostructuring of carbon materials by means of a calcium phosphate template

P. Gibot<sup>1</sup> · F. Schnell<sup>1</sup> · M. Schaefer<sup>1</sup> · D. Spitzer<sup>1</sup>

Published online: 6 September 2018  
© Springer Science+Business Media, LLC, part of Springer Nature 2018

## Abstract

Nanostructured porous carbon powders were elaborated by means of a hard-template approach, using environmentally friendly materials such as sucrose and  $\text{Ca}_3(\text{PO}_4)_2$  tricalcium phosphate hydrate as carbon and template sources, respectively. While the naturally occurring carbohydrate is widely used for carbon materials synthesis, the tricalcium phosphate was never suggested as template despite its efficiency as shown in the present study. The resulting carbon materials were characterized by elemental analysis, Raman spectroscopy, nitrogen adsorption and electron microscopies. Porous carbon powders with disordered hierarchical porous structure, exhibiting tunable textural properties (specific surface areas, pore volume...), were thus synthesized. For instance, with a template/carbon precursor weight ratio of 1, the specific surface area and pore volume were significantly increased compared to the counterpart which was elaborated without a  $\text{Ca}_3(\text{PO}_4)_2$  template. The ease of implementation coupled to the low cost of different reagents make the present process potentially competitive for synthesizing porous carbon powders.

**Keywords** Carbon ·  $\text{Ca}_3(\text{PO}_4)_2$  · Template · Nanostructuring · Textural properties

## 1 Introduction

To date, carbon material is undoubtedly one of the most studied materials because of its exceptional physicochemical properties which allow it to be considered as a promising candidate in a large number of applications in fields as varied as (opto)electronic, mechanic, electrochemistry, biomedical,

for hydrogen storage, catalysis, and many more. Among these unique characteristics, a good thermal stability under oxidizing atmosphere, chemical resistance against numerous aggressive agents and high melting and sublimation points can be pointed out. The existence of the various natural allotropic forms (amorphous, graphite and diamond) associated with the mostly synthetic forms (fullerenes, nanotubes or graphene) make carbon a material with numerous facets. For instance, carbon can exhibit opposite thermal and electrical properties; i.e. insulating and conducting, different mechanical properties (hardness, lubricating) and very distinct optical properties (wide range of refractive indexes) all that as function of the crystallographic hybridization exhibited [1–3].

Among the aims of the studies regularly mentioned in the literature regarding carbon material, the possibility of tailoring a material with specific and well defined textural properties (specific surface area, pore volume, pore size...) appears to be the most worrying topic for many researchers. Indeed, the performance of the carbon material in highly valued applications such as for instance catalysis, filtration/separation and energy storage (hydrogen) strongly depends on these properties. Carbon materials with defined porosity (micro-, meso- and macroscale) can be synthesized by means of the well-known templating method where a wide variety

**Electronic supplementary material** The online version of this article (<https://doi.org/10.1007/s10934-018-0672-6>) contains supplementary material, which is available to authorized users.

✉ P. Gibot  
pierre.gibot@isl.eu

F. Schnell  
fabien.schnell@isl.eu

M. Schaefer  
michael.schaefer@isl.eu

D. Spitzer  
denis.spitzer@isl.eu

<sup>1</sup> Laboratoire des Nanomatériaux pour Systèmes Sous Sollicitations Extrêmes (NS3E), CNRS/ISL/UNISTRA UMR 3208, Institut franco-allemand de recherches de Saint-Louis (ISL), 5 rue du Général Cassagnou, BP 70034, 68301 Saint-Louis, France

of template agents (organic, and inorganic or polymer species) are used to precisely tailor the textural properties [4]. In a non-exhaustive way, some of them can be cited. Firstly, soft templates may be used such as (i) the poly(alkylene oxide) symmetric triblock copolymers (PEO–PPO–PEO as Pluronic P123 and F127) [5, 6] and (ii) the asymmetric diblock copolymers as the polystyrene-*block*-polyvinylpyridine (PS-*b*-P4VP) [7] and the poly(styrene)-*block*-poly(ethylene oxide) (PS-*b*-PEO) [8] mixed with resorcinol/formaldehyde, phenolic resin and resol as carbon sources. The fact that this approach is time-consuming and that carbon precursors are toxic represent real drawbacks to an industrial development. Secondly, among the hard templates, the silica-based mesoporous materials (MCM-48, SBA-15, KIT-6, MSU-H, MSU-1, HMS) [9–14], zeolites [15–17] and monodispersed colloidal silica dispersions ( $\text{SiO}_2$ ) are often mentioned to synthesize ordered (but not systematically) porous carbon from propylene, mesophase pitch, resorcinol/formaldehyde and sucrose as carbon precursors [10, 18–20]. Silica templates have been substituted by other oxides such as titanium oxide ( $\text{TiO}_2$ ) or zirconium oxide ( $\text{ZrO}_2$ ) for similar results [21, 22]. Yet, the fact that toxic hydrofluoric acid is needed for the removal of the oxide templates may be seen as a major challenge for an up-scaling of the process. To bypass this problem, more readily removal colloidal dispersions or nanoparticles were tested such as the following ones based on zinc oxide (ZnO) and magnesium oxide (MgO) leading to aperiodic hierarchical porous structures [23, 24]. More recently, Xu et al. have reported the use of a  $\text{CaCO}_3$  calcium carbonate template, a biomaterial, as suitable hard template to synthesize mesoporous carbon materials [25].

In the present work, we report a simple and efficient method for the preparation of amorphous carbon materials exhibiting a tunable hierarchical porosity highly efficient in catalysis field [26]. This process is based on the pyrolysis of a classical carbon source (sucrose) previously mixed with calcium phosphate as surface generating agent. Since the calcium phosphate material presents some advantages such as being environmentally friendly, a commercial availability at micron- to nanoscale and readily removal, the current approach can be seen as an interesting alternative to the development of the hard-templated process amply used for the nanostructuring of carbon materials. The as-made carbon materials were characterized by means of usual laboratory techniques.

## 2 Experimental section

Sucrose ( $\text{C}_{12}\text{H}_{22}\text{O}_{11}$ , reagent grade) and tricalcium phosphate hydrate ( $\text{Ca}_3(\text{PO}_4)_2 \cdot x\text{H}_2\text{O}$ , reagent grade) were purchased from Sigma Aldrich while hydrochloric acid (HCl, 37%) was obtained from Prolabo. All chemicals were used without any further purification.

Typically the synthesis process of high specific surface areas carbon materials inspired from [27, 28], where the use of calcium phosphate was successfully proposed to nanostructure polymer and ceramic, can be described as follows: 0.5 g of sucrose was dissolved in 50 mL of distilled water. Then, a precise amount of tricalcium phosphate hydrate particles was added and the resulting mixture was stirred and sonicated (1 h) to get a homogeneous suspension. The amount of tricalcium phosphate hydrate was adjusted in order to obtain a  $[\text{Ca}_3(\text{PO}_4)_2 \cdot x\text{H}_2\text{O}/\text{sucrose}]$  weight ratio of 1/3, 2/3 and 1. The resulting mixtures, deposited into porcelain crucibles, were pre-treated at 250 °C in air (2 h) and at 700 °C under argon (2 h) yielding the preparation of blackish [template/carbon] composites. This pyrolysis temperature was selected because of the textural properties of the carbon material were optimal in these conditions. For higher temperatures, a collapse of the porosity seems to occur (not shown and discussed here). After hand-milling in a mortar, the composites were emerged in diluted hydrochloric acid (1 M) to remove the calcium salt. The products were centrifuged and washed several times with distilled water and once with acetone. The as-prepared carbon materials were dried at 80 °C and were designated as  $\text{C}_{\text{suc-x}}$  where, suc represents the carbon source (sucrose) and x the  $[\text{Ca}_3(\text{PO}_4)_2 \cdot x\text{H}_2\text{O}/\text{sucrose}]$  weight ratio. X was fixed at zero for carbon prepared without template. Considering our experimental conditions, the yield of carbon from sucrose was 25 wt%.

Simultaneous thermogravimetric and differential thermal analyses (TG–DTA) were performed on the as-prepared carbon materials by means of an Exstar 6000 apparatus (Seiko, Japan). The thermal behaviours of the samples were recorded under air (100 mL/min) between 25 and 800 °C with a heating rate of 10 °C/min and by using an open alumina pan. The chemical composition (C, H, O) of the materials were determined by burning under a helium/oxygen flow at 1050 °C. The gaseous products ( $\text{CO}_2$ ,  $\text{H}_2\text{O}$ ...) were separated on a chromatographic column and quantified by using a thermal conductivity detector. The structure of the as-prepared carbon materials was determined with an InVia confocal Raman microscope (Renishaw, United Kingdom) equipped with an argon ion laser ( $\lambda = 514$  nm), a  $\times 50$  objective and calibrated with a Si crystal before analysis. The spectra were acquired in the range of 500–2500  $\text{cm}^{-1}$  with an exposure time of 50 s. under a laser power ( $P = 25$  mW) set at 5%. The OriginPro Vers.9 software (OriginLab Corp., USA) was used to fit the different spectra considering Gaussian functions. The textural properties of the samples were determined by nitrogen ( $\text{N}_2$ ) physisorption measurements at  $-196$  °C performed on an Accelerated Surface Area and Porosimetry 2020 analyzer (Micromeritics, USA). Prior to the analysis, the samples were outgassed at 250 °C under vacuum for 6 h. The BET equivalent areas ( $a_{\text{BET}}$ ) were determined according to the Brunauer–Emmet–Teller (BET) method in the 0.005–0.10 relative pressure range [29]. The total pore volume ( $V_p$ ) were

estimated from the volumes of nitrogen adsorbed at a relative pressure  $P/P_0$  of 0.99. The Harkins–Jura  $t$ -plot model, applied to the adsorption branch of the isotherms, was used to determine the micropore areas ( $a_{\mu\text{m}}$ ) and the micropore volumes ( $V_{\mu\text{m}}$ ) of the different samples [30]. The external surface areas ( $a_e$ ) and the meso/macroporous volumes were calculated as the differences between  $a_{\text{BET}}$  and  $a_{\mu\text{m}}$  and  $V_p$  and  $V_{\mu\text{m}}$ , respectively. The pore size distributions (PSD) were determined from the adsorption branches by means of the Barrett–Joyner–Halenda (BJH) method. The microstructure and particle sizes of the materials were observed with a Nova Nano-SEM 450 scanning electron microscope (SEM) (FEI™, USA) and a CM 200 transmission electron microscope (Philips, USA) operating at 10 kV and 200 kV, respectively.

### 3 Results and discussion

Figure 1 shows the TG–DTA curves of the carbon samples obtained after removal of the  $\text{Ca}_3(\text{PO}_4)_2 \cdot x\text{H}_2\text{O}$  particles of the [template/carbon] composites. All TG curves are similar with two weight losses recorded before 200 °C featuring to the removal of surface water molecules and around 450–650 °C that may be interpreted by the oxidation of carbon species. By correlation, endothermic and exothermic phenomena were recorded, respectively, in the same temperatures ranges on the DTA curves for each sample. For all investigated samples, the weight loss being higher than 95% suggests a high gasification of the products and consequently the quasi-absence of the mineral template, normally stable under these experimental conditions [31]. As a reminder, the weight amount of tricalcium phosphate hydrate in the [template/carbon] composites ranges from 57 to 80% for the composites prepared with a  $[\text{Ca}_3(\text{PO}_4)_2 \cdot \text{H}_2\text{O}/\text{sucrose}]$  weight ratio of 1/3, 2/3 and 1, respectively.

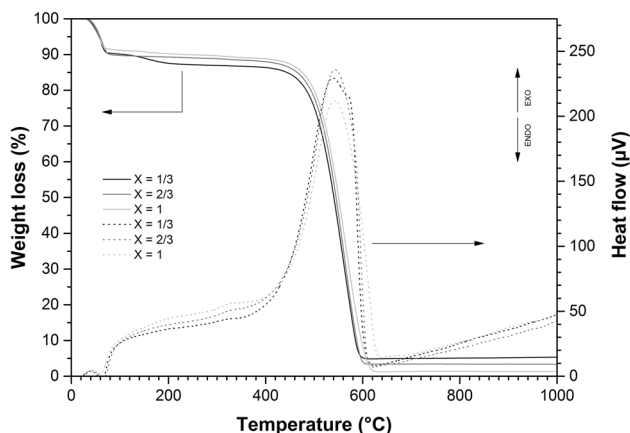


**Fig. 1** TG–DTA curves of the hard-templated carbon materials with  $\text{Ca}_3(\text{PO}_4)_2 \cdot x\text{H}_2\text{O}$  particles as template. ( $C_{\text{suc-}x}$  with  $x = [\text{Ca}_3(\text{PO}_4)_2 \cdot x\text{H}_2\text{O}/\text{sucrose}]$ )

This result shows the efficiency of the washing with diluted acid to remove the template that is incontestably a real advantage on the most traditional templates such as mesoporous silica, alumina membranes, zeolites and so on, used for nanostructuring materials which need the use of toxic hydrofluoric acid for a long period of time for their removal.

The elemental compositions of the as-obtained carbon samples are gathered in Table 1. As it can be noticed, the main chemical components are carbon, hydrogen and oxygen. The presence of the two last elements suggests an incomplete carbonization of the carbon precursor according to the above-given experimental conditions that may be explained by the applied pyrolysis temperature which is slightly lower than 900 °C classically used for the synthesis of pure carbon matrices from sucrose as precursor [9, 10, 12]. The differences in the total elemental compositions ( $\Sigma$ ) recorded for two of the templated carbon materials synthesized with  $X = 1/3$  ( $C_{\text{suc-}1/3}$ ) and  $2/3$  ( $C_{\text{suc-}2/3}$ ) with the centesimal composition are in good agreement and in the same level of magnitude with the gravimetric data presented in Fig. 1 where residual products are observed after an oxidative treatment.

Figure 2 shows the Raman spectra of the different as-synthesized carbon samples. All spectra are similar and present two main peaks located at  $1597 \text{ cm}^{-1}$  and  $1342 \text{ cm}^{-1}$  known as being the G and D bands, respectively, of a graphitic (G) carbon material exhibiting some disorders or defects (D) in its structure [32]. The G-band characterizes the vibrations in the planes of the graphene layers while the D-band corresponds to the defects in the graphene edges. The fitting of the carbon material prepared without the use of a template is presented in insert of Fig. 2. The better fitting parameters were obtained with a Gaussian-based fit where a correlation coefficient ( $r^2$ ) of 0.994 was got. In our case, as it can be seen, this result was determined from a multipeak fit, in opposite to the classical two-peaks method (G and D bands), which may be explained by the amorphous or high disordered character of the investigated material [32]. The two supplementary peaks were chosen around  $1200 \text{ cm}^{-1}$  and  $1540 \text{ cm}^{-1}$ .

In the literature, the D/G intensity ratio is largely used to determine the structural arrangement or graphitization

**Table 1** Chemical compositions of the carbon materials synthesized by means of  $\text{Ca}_3(\text{PO}_4)_2 \cdot x\text{H}_2\text{O}$  particles as template ( $C_{\text{suc-}x}$  with  $x = [\text{Ca}_3(\text{PO}_4)_2 \cdot x\text{H}_2\text{O}/\text{sucrose}]$  weight ratio)

	C (wt%)	O (wt%)	H (wt%)	$\Sigma$
$C_{\text{suc-}0}$	92.7	5.8	1.5	100
$C_{\text{suc-}1/3}$	85.7	6.1	1.5	93.3
$C_{\text{suc-}2/3}$	88.3	5.3	1.3	94.9
$C_{\text{suc-}1}$	93.0	5.1	1.3	99.4

Amounts calculated by elemental analysis (EA)

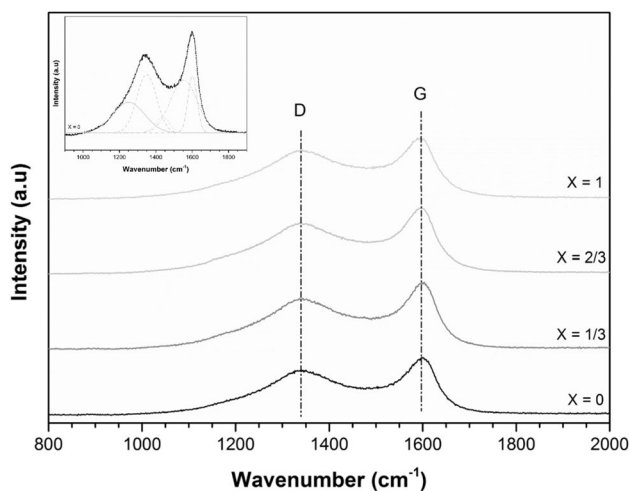


**Fig. 2** Raman spectra of the hard-templated carbon materials with  $\text{Ca}_3(\text{PO}_4)_2 \cdot x\text{H}_2\text{O}$  particles as template ( $\text{C}_{\text{suc}-x}$  with  $x = [\text{Ca}_3(\text{PO}_4)_2 \cdot x\text{H}_2\text{O}/\text{sucrose}]$ )

degree of the material; a high ratio characterizes a material with a lot of defects whereas a low ratio is obtained for a high ordered sample as the pure graphite. In the present work, the D/G ratio, based on the fittings, is close to 1.1 for all carbon samples prepared with the use or not of  $\text{Ca}_3(\text{PO}_4)_2 \cdot x\text{H}_2\text{O}$  tricalcium phosphate hydrate—independent of the used amount of template. This value emphasizes a high structural disorder or low graphitization degree of the as-synthesized carbons, which is totally in agreement with X-ray diffraction analysis (Supporting Information 1) [33]. By this characterization technique, the formation of amorphous carbon materials has been observed, as suggested from the absence of reflections of graphite within the investigated angular range. The latter is consistent with the low applied pyrolysis temperature of 700 °C.

The textural properties of the carbon materials were studied by nitrogen sorption measurements performed at  $-196$  °C. Figure 3a represents the nitrogen isotherms of the samples prepared with the  $\text{Ca}_3(\text{PO}_4)_2 \cdot x\text{H}_2\text{O}$  template with a weight ratio (X) ranging from 1/3 to 1. The nitrogen isotherm of the sample synthesized without the assistance of the calcium-based template ( $\text{C}_{\text{suc}_0}$ ), voluntarily omitted in the Fig. 3a for clarity, is classic of a microporous material with a type I profile (Supporting Information 2). The different hard-templated carbonaceous samples exhibit *composite isotherms* which can be interpreted as the sum of type I and type II isotherms typically used to characterize microporous and large mesoporous or macroporous samples, respectively, according to the IUPAC classifications. For all samples, the adsorption branches can be decomposed as follows: (i) micropores filling for relative pressures ( $P/P_0$ ) lower than 0.05, (ii) mono- and multimolecular adsorption between 0.05–0.10 and 0.10–0.95 relative pressures, respectively and finally (iii) capillary condensation

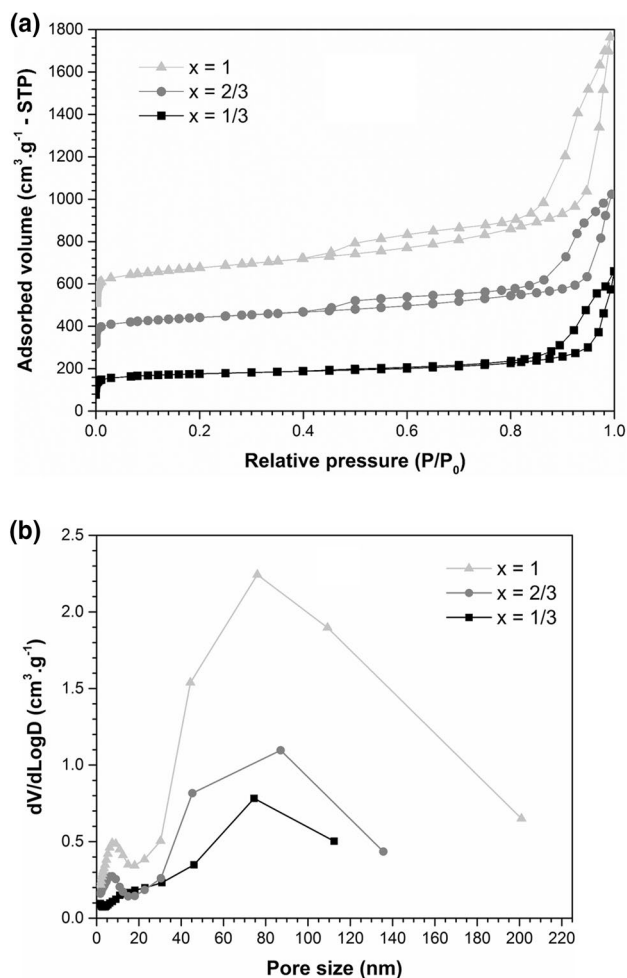


**Fig. 3** **a** Nitrogen gas sorption isotherms and **b** pore size distributions of the hard-templated carbon materials with  $\text{Ca}_3(\text{PO}_4)_2 \cdot x\text{H}_2\text{O}$  particles as template ( $\text{C}_{\text{suc}-x}$  with  $x = [\text{Ca}_3(\text{PO}_4)_2 \cdot x\text{H}_2\text{O}/\text{sucrose}]$ ) (The isotherms curves were shifted to the ordinate axis for a better legibility)

without horizontal plateau above 0.95  $P/P_0$ . From the nitrogen desorption stage, from the samples surfaces, the formation of a Type H3 hysteresis loops (non-covering of desorption and adsorption branches) is observed in each case. It is synonym of a porosity originated of a non-rigid structure as for instance an assembling of aggregates and also of macropores which are not completely filled with pore condensate. As it can be seen, the higher the  $[\text{Ca}_3(\text{PO}_4)_2 \cdot x\text{H}_2\text{O}/\text{sucrose}]$  weight ratio (X) is, the larger the hysteresis loop becomes, suggesting that the porosity of the carbon materials continually increases with X.

Table 2 gathers the textural data derived from the nitrogen isotherms and for which ones the coherence tests were systematically verified which is essential for materials exhibiting micropores [29]. The carbon materials display BET equivalent areas ( $a_{\text{BET}}$ ) ranging from 516  $\text{m}^2/\text{g}$  ( $\text{C}_{\text{suc}_0}$ ) to 824  $\text{m}^2/\text{g}$  ( $\text{C}_{\text{suc}_1}$ ) with a rapid increase from the use of calcium-based template (662  $\text{m}^2/\text{g}$  for  $\text{C}_{\text{suc}_{1/3}}$ ). As it can be seen, the part of the external surface area ( $a_1$ ), area on which

**Table 2** Textural properties of the hard-templated carbon materials prepared by means of  $\text{Ca}_3(\text{PO}_4)_2 \cdot x\text{H}_2\text{O}$  particles as template ( $\text{C}_{\text{suc}-x}$  with  $x = [\text{Ca}_3(\text{PO}_4)_2 \cdot x\text{H}_2\text{O}/\text{sucrose}]$  weight ratio)

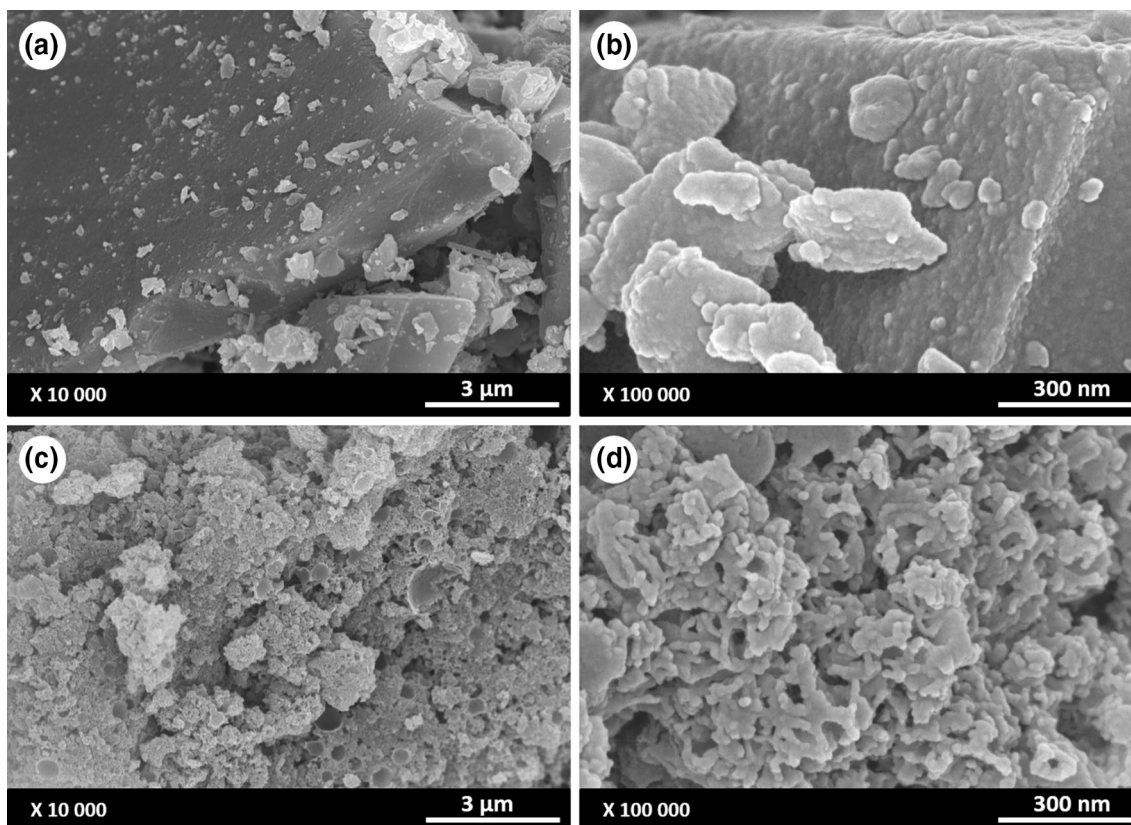
Sample	Surface area ( $\text{m}^2/\text{g}$ )			Pore volume ( $\text{cm}^3/\text{g}$ )		
	$a_{\text{BET}}$	$a_t$	$a_{\mu\text{m}}$	$V_p$	$V_{\mu\text{m}}$	$V_{\text{meso/macro}}$
$\text{C}_{\text{suc}-0}$	516	17	499	0.22	0.19	–
$\text{C}_{\text{suc}-1/3}$	662	132	530	1.02	0.21	0.81
$\text{C}_{\text{suc}-2/3}$	713	283	430	1.20	0.18	1.02
$\text{C}_{\text{suc}-1}$	824	482	342	2.04	0.15	1.91

a multimolecular layer can be form (pores size  $> 2$  nm; i.e. mesopores and macropores), increases with the amount of template to the detriment of the micropores area ( $a_{\mu\text{m}}$ ). These two behaviors are synchronized and attributed to the removal of calcium-based template initially embedded in the carbon powder because sucrose amount is constant for all samples. The formation of pores with size  $> 2$  nm ( $a_t$ 's increase) can be explained by the template particle itself since its size is ranged from 10 to 120 nm (Supporting Information 2) while the decrease of the micropore area ( $a_{\mu\text{m}}$ ) might come about the association of micropores, neighbors of template particles, thus creating meso- and macropores.

Regarding the value of the micropore volume ( $V_{\mu\text{m}}$ ), negligible changes are noticed for the different templated carbon materials that lead to discard all responsibility of the

template in its formation. As classically mentioned in the literature, the micropore volume is originated by the releasing of small gaseous molecules (e.g.  $\text{H}_2\text{O}$ ,  $\text{CH}_4$ ,  $\text{CO}$ ,  $\text{CO}_2 \dots$ ) during the pyrolysis of the sucrose reagent [34]. Thus, the  $\text{Ca}_3(\text{PO}_4)_2 \cdot x\text{H}_2\text{O}$  nanoparticles can be considered as effective regarding the development of high surface materials exhibiting large pores. The evidence of the presence of multiscale pore sizes in these porous carbon samples is given by the BJH adsorption pore size distributions shown in Fig. 3b. The different curves, with Gaussian profiles and centered around 70–80 nm in all cases, exhibit very large pore size distributions ranging from 20 to 200 nm agrees with the presence of mesopores and macropores, respectively.

Figure 4a–d show the SEM images of two porous carbons synthesized without and with the use of  $\text{Ca}_3(\text{PO}_4)_2 \cdot x\text{H}_2\text{O}$

**Fig. 4** SEM images of the carbon materials prepared without (a, b) and with  $\text{Ca}_3(\text{PO}_4)_2 \cdot x\text{H}_2\text{O}$  particles as template (c, d) ( $x = [\text{Ca}_3(\text{PO}_4)_2 \cdot x\text{H}_2\text{O}/\text{sucrose}] = 1$ )

template. The carbon material prepared by pyrolysis of sucrose at 700 °C is presented in Fig. 4a, b. At low magnification, the material is made of particles with an undefined morphology. The size of the particles ranges from sub-micrometer to some micrometers. At higher magnification, the surface of these large particles is not flat but it can be noticed a real roughness of the particles. More, smaller particles are observed at the surface of the biggest ones, which may be at the origin of the specific surface developed by the powder. Figure 4c, d present the morphology of the carbon sample synthesized in the presence of  $\text{Ca}_3(\text{PO}_4)_2 \cdot x\text{H}_2\text{O}$  template with an X weight ratio of about 1.

From the low magnification, it can be obviously seen that the use of tricalcium phosphate hydrate has a significant effect on the microstructural aspect of the carbon material. Drastic changes are noted, in particular in the particle sizes and in the apparent porosity of the bulk. The hard-templated carbon (Fig. 4c) consists of smaller particles with a trend to agglomeration, due to their small dimension, but keeping a high interparticular porosity as can be clearly seen. This microstructural aspect may be put in parallel with the fact that in the case where the carbon material is prepared with the inorganic template, the powder is crumblier and looser. Moreover, from a careful observation of the present image, spherical prints are seen at some places. These prints correspond in morphology and size (10–120 nm) to the  $\text{Ca}_3(\text{PO}_4)_2 \cdot x\text{H}_2\text{O}$  particles used to nanostructure the carbon powder (Supporting Information 2). At higher magnification (Fig. 4d), the carbon particles exhibit an average size ranging from 20 to 30 nm, with a narrow particle size distribution contrary to the sample prepared without template (Fig. 4b), and a coalescence is noticed. Finally, this hard-templated carbon material shows a complex architecture where the porosity is predominant. The SEM observations are plenty consistent with the nitrogen sorption measurements and the TG–DTA analyses, previously discussed, in the sense where they confirm the porous character of the as-synthesized carbon powders and explain why it may be difficult to eliminate totally the template in such complicated architectures (cf. Fig. 1).

Figure 5 displays TEM images of the porous carbon prepared by means of a calcium-based template ( $\text{C}_{\text{suc}_1}$ ).

The carbon material is represented, in a long scale, by muddled thin layers coupled to a disordered porous structure (Fig. 5a). The pores are omnipresent and uniformly distributed within the porous carbon network. The pore size distribution is large; i.e. from nano- to submicrometer size, which is in agreement with the dimension of the  $\text{Ca}_3(\text{PO}_4)_2 \cdot x\text{H}_2\text{O}$  nanoparticles used as template (Supporting Information) and with the nitrogen sorption measurements discussed above. At higher magnification (Fig. 5b), no crystallographic order is observed within the carbon layers which is consistent with the Raman characterization, also discussed in this paper.

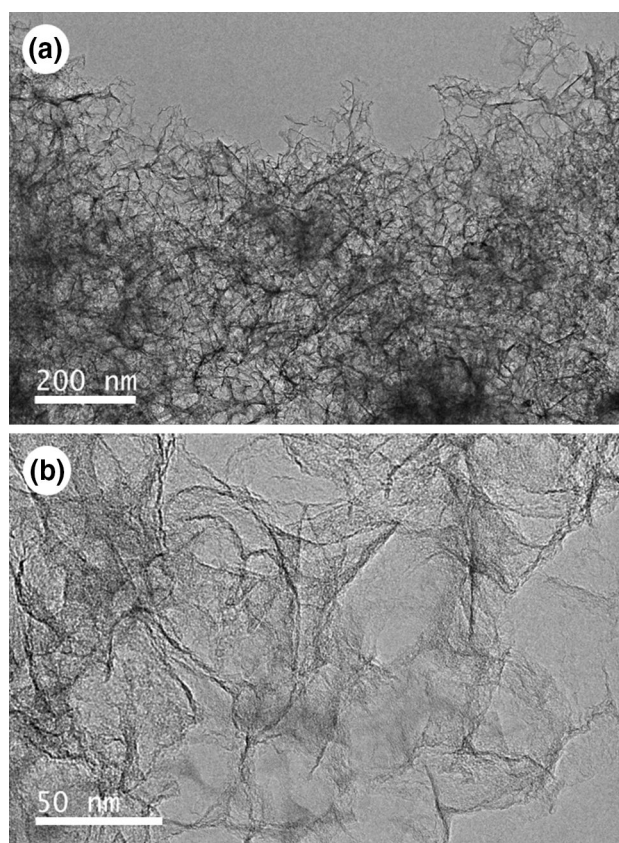


**Fig. 5** TEM images at **a** low and **b** high magnification of the carbon material prepared with  $\text{Ca}_3(\text{PO}_4)_2 \cdot x\text{H}_2\text{O}$  particles as template ( $x = [\text{Ca}_3(\text{PO}_4)_2 \cdot x\text{H}_2\text{O}/\text{sucrose}] = 1$ )

Based on the previous observations obtained from the different characterizations techniques used (Raman spectroscopy, nitrogen adsorption, SEM and TEM analyses), an attempt of mechanism regarding the formation of the porous carbon material is suggested in Fig. 6. Typically, the process displays in the present work rest on the formation of carbon/ $\text{Ca}_3(\text{PO}_4)_2 \cdot x\text{H}_2\text{O}$  composites originated from the following steps:  $\text{Ca}_3(\text{PO}_4)_2 \cdot x\text{H}_2\text{O}$  particles are poured in a distilled water solution where sucrose molecules have been previously solubilized. The resulting suspension, kept at room temperature for a defined duration, results in evaporation of water solvent and thus re-precipitation of sucrose on the surface of the  $\text{Ca}_3(\text{PO}_4)_2 \cdot x\text{H}_2\text{O}$  particles. The pyrolysis step conducted after that, lead to the formation of black (carbon/tricalcium phosphate) composites where Ca-based particles are embedded in carbon matrices, thermal decomposition products of sucrose, exhibiting a microporosity explained by the removal of small molecules [34]. Finally, the calcium-based template particles are removed from the carbon matrices, via an acidic etching, releasing a second kind of porosity rather ranged from meso- to submicron scale. Evidence for the embedding of the template particles in the carbon matrices is provided by the examination carried out by SEM

**Fig. 6** Suggested mechanism for the preparation of porous carbon powder by means of  $\text{Ca}_3(\text{PO}_4)_2 \cdot x\text{H}_2\text{O}$  biomaterial as template

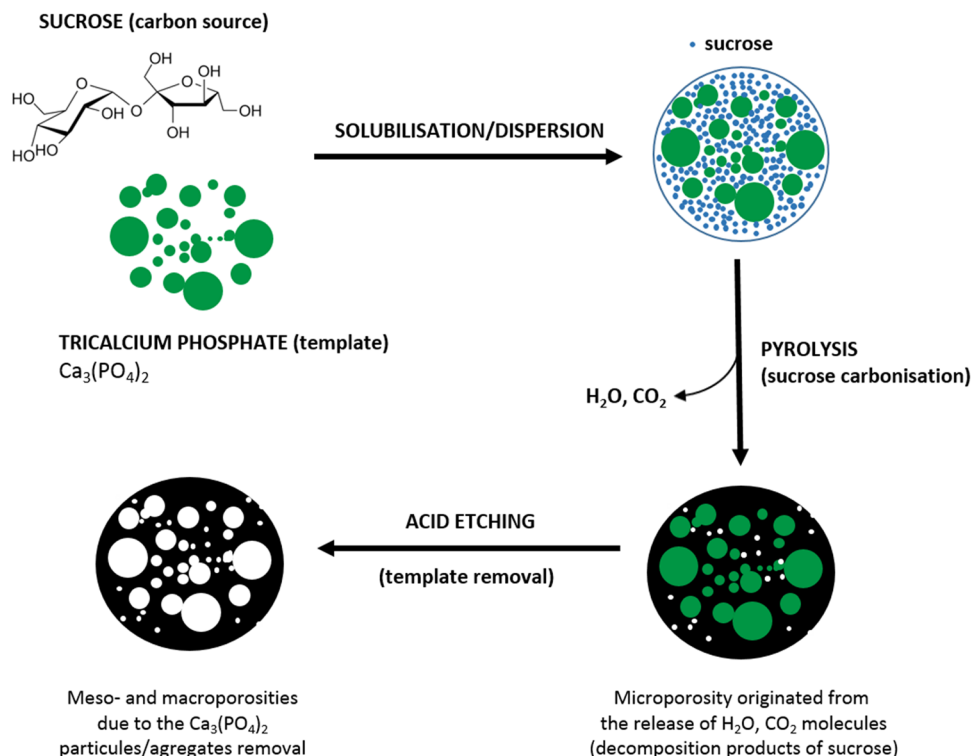


(Fig. 4c) where a lot of spherical imprints with a large size distribution are observed, after acid etching, what is a perfect duplication of the tricalcium phosphate particles used as template (Supporting Information 3). The dependence of the textural properties (specific surface area and porosity) at high scale with the template particles is obvious (Table 2) since meso and macro-porosities increase with the template amount.

## 4 Conclusion

The synthesis of carbon powders with a disordered multi-scale porous structure was achieved through a hard-template method with sucrose as carbon source and the assistance of an mineral template  $\text{Ca}_3(\text{PO}_4)_2 \cdot x\text{H}_2\text{O}$  tricalcium phosphate hydrate. The resulting carbon sample exhibits textural properties directly correlated to the amount of template used. For instance, with a  $[\text{Ca}_3(\text{PO}_4)_2 \cdot x\text{H}_2\text{O}/\text{sucrose}]$  weight ratio of 1, the carbon material is characterized by a specific surface area and pore volume of  $833 \text{ m}^2/\text{g}$  and  $2.07 \text{ cm}^3/\text{g}$ , respectively, which is much more higher than the values of this counterpart prepared without the assistance of the template ( $456 \text{ m}^2/\text{g}$ ,  $0.19 \text{ cm}^3/\text{g}$ ). The template used reveals following advantages: non-toxicity, high thermal stability and readily removal by diluted acid solutions. It could be proved to be a serious alternative for synthesizing porous carbon powders of interest for energy

applications (hydrogen storage, supercapacitors, metal–ion batteries) or heterogeneous catalysis where the nanoscale and the porosity are key factors. The use of tricalcium phosphate nanoparticles dispersions with a narrow particles size distribution and without aggregation phenomena (surface functionalization) would improve the efficiency of this approach specifically in the synthesis of carbon materials with ordered and tailored textural properties.

**Acknowledgements** The authors express their grateful thanks to S. Adach (SRSMC, University of Lorraine, France), L. Vidal (IS2M, University of Mulhouse, France) and H. Nouali (IS2M, University of Mulhouse, France) for the elemental chemical analyses, the transmission electron microscopy observations and the wise advices regarding the textural properties of materials, respectively.

## Compliance with ethical standards

**Conflict of interest** The authors declare that they have no conflict of interest.

## References

1. P. Bernier, S. Lefrant, *Le carbone dans tous ses états*, 1st edn. (Gordon and Breach, Amsterdam, 1997)
2. P. Delhaes, *Solides et matériaux carbonés (3 volumes)* (Hermes Science Publications, Paris, 2009)
3. K.D. Sattler, *Carbon Nanomaterials Sourcebook—Graphene, Fullerenes, Nanotubes and Nanodiamonds*, 1st edn. (CRC Press, Boca Raton, 2016)

4. J. Tang, J. Liu, N.L. Torad, T. Kimura, Y. Yamauchi, *Nano Today* **9**, 305–323 (2014)
5. F.Q. Zhang, Y. Meng, D. Gu, Y. Yan, C.Z. Yu, B. Tu, D.Y. Zhao, *J. Am. Chem. Soc.* **127**, 13508–13509 (2005)
6. J. Li, Y. Jia, W. Wang, L. Song, G. Zhu, *J. Porous Mater.* **25**, 771–777 (2018)
7. C.D. Liang, K.L. Hong, G.A. Guiochon, J.W. Mays, S. Dai, *Angew. Chem. Int. Ed.* **43**, 5785–5789 (2004)
8. Y.H. Deng, Y. Cai, Z.K. Sun, D. Gu, J. Wei, W. Li, X.H. Guo, J.P. Yang, D.Y. Zhao, *Adv. Funct. Mater.* **20**, 3658–3665 (2010)
9. R. Ryoo, S.H. Joo, S. Jun, *J. Phys. Chem. B* **103**, 7743–7746 (1999)
10. J. Parmentier, S. Saadhallah, M. Reda, P. Gibot, M. Roux, L. Vidal, C. Vix-Guterl, J. Patarin, *J. Phys. Chem. Solids* **65**, 139–146 (2004)
11. G. Gupta, D.A. Slanac, P. Kumar, J.D. Wiggins-Camacho, J. Kim, R. Ryoo, K.J. Stevenson, K.P. Johnston, *J. Phys. Chem. C* **114**, 10796–10805 (2010)
12. S.S. Kim, T.S. Pinnavaia, *Chem. Commun.* **0**, 2418–2419 (2001)
13. S. Alvarez, S.A.B. Fuertes, *Carbon* **42**, 433–436 (2004)
14. J. Lee, S. Yoon, S.M. Oh, S. Shin, T. Hyeon, *Adv. Mater.* **12**, 359–363 (2000)
15. T. Kyotani, T. Nagai, S. Inoue, A. Tomita, *Chem. Mater.* **9**, 609–615 (1997)
16. Z. Ma, T. Kyotani, A. Tomita, *Carbon* **40**, 2367–2374 (2002)
17. K. Matsuoka, Y. Yamagishi, T. Yamazaki, N. Setoyama, A. Tomita, T. Kyotani, *Carbon* **43**, 876–879 (2005)
18. S. Han, T. Hyeon, *Chem. Commun.* **19**, 1955–1956 (1999)
19. S. Kang, J.S. Yu, M. Kruk, M. Jaroniec, *Chem. Commun.* **16**, 1670–1671 (2002)
20. Z.B. Lei, Y. Xiao, L.Q. Dang, M. Lu, W.S. You, *Microporous Mesoporous Mater.* **96**, 127–134 (2006)
21. C. de Almeida Filho, A.J.G. Zarbin, *Carbon* **44**, 2869–2876 (2006)
22. B.L. Su, A. Vantomme, L. Surahy, R. Pirard, J.P. Pirard, *Chem. Mater.* **19**, 3325–3333 (2007)
23. H.-y. Liu, Z.-b. Feng, J. Wang, J.-y. Diao, D.-s. Su, *New Carbon Mater.* **31**, 87–91 (2016)
24. T. Morishita, Y. Soneda, T. Tsumura, M. Inagaki, *Carbon* **44**, 2360–2367 (2006)
25. B. Xu, L. Peng, G. Wang, G. Cao, F. Wu, *Carbon* **48**, 2361–2380 (2010)
26. M. Choi, K. Na, J. Kim, J.Y. Sakamoto, O. Terasaki, R. Ryoo, *Nature* **461**, 246–249 (2009)
27. P. Gibot, F. Schnell, D. Spitzer, *Mater. Lett.* **161**, 172–174 (2015)
28. P. Gibot, F. Schnell, D. Spitzer, *Microporous Mesoporous Mater.* **219**, 42–47 (2016)
29. J. Rouquerol, P. Llewellyn, F. Rouquerol, *Stud. Surf. Sci. Catal.* **160**, 49–56 (2007)
30. F. Rouquerol, J. Rouquerol, K.S.W. Sing, P. Llewellyn, G. Maurin, *Adsorption by Powders and Porous Solids*, 2nd edn. (Academic Press, London, 1999)
31. N. Matsumoto, K. Yoshida, K. Hashimoto, Y. Toda, *Mater. Res. Bull.* **44**, 1889–1894 (2009)
32. A.C. Ferrari, J. Robertson, *Phys. Rev. B* **61**, 14095–14107 (2000)
33. B. Wopenka, Y.C. Xu, E. Zinner, S. Amari, *Geochim. Cosmochim. Acta* **106**, 463–489 (2013)
34. M. Inagaki, F. Kang, *Materials Science and Engineering of Carbon: Fundamentals*, 2nd ed., chap. 2 (Tsinghua University Press Limited, Elsevier Inc., Oxford, 2014)